Title
Microfluidic Strategies for Understanding the Mechanics of Cells and Cell-Mimetic Systems

Journal
Annual Review of Chemical and Biomolecular Engineering, 6(1)

ISSN
1947-5438

Authors
Dahl, Joanna B
Lin, Jung-Ming G
Muller, Susan J
et al.

Publication Date
2015-07-24

DOI
10.1146/annurev-chembioeng-061114-123407

Peer reviewed

Microfluidic Strategies for Understanding the Mechanics of Cells and Cell-Mimetic Systems

Joanna B. Dahl,[1,*] Jung-Ming G. Lin,[2,3,*] Susan J. Muller,[1] and Sanjay Kumar[2,3]

[1]Department of Chemical and Biomolecular Engineering, [2]Department of Bioengineering, and [3]UC Berkeley/UCSF Graduate Program in Bioengineering, University of California, Berkeley, California 94720; email: skumar@berkeley.edu

Annu. Rev. Chem. Biomol. Eng. 2015. 6:293–317

First published online as a Review in Advance on July 2, 2015

The *Annual Review of Chemical and Biomolecular Engineering* is online at chembioeng.annualreviews.org

This article's doi: 10.1146/annurev-chembioeng-061114-123407

*Authors contributed equally to this work

Keywords

particles, droplets, capsules, vesicles, migration, chemotaxis

Abstract

Microfluidic systems are attracting increasing interest for the high-throughput measurement of cellular biophysical properties and for the creation of engineered cellular microenvironments. Here we review recent applications of microfluidic technologies to the mechanics of living cells and synthetic cell-mimetic systems. We begin by discussing the use of microfluidic devices to dissect the mechanics of cellular mimics, such as capsules and vesicles. We then explore applications to circulating cells, including erythrocytes and other normal blood cells, and rare populations with potential disease diagnostic value, such as circulating tumor cells. We conclude by discussing how microfluidic devices have been used to investigate the mechanics, chemotaxis, and invasive migration of adherent cells. In these ways, microfluidic technologies represent an increasingly important toolbox for investigating cellular mechanics and motility at high throughput and in a format that lends itself to clinical translation.

INTRODUCTION

Although biologists have long understood that soluble signals, such as growth factors and hormones, can strongly influence cell behavior, it has become increasingly clear over the past two decades that cells can also sense physical cues in their environment. For example, local tissue mechanics and geometry can drive a wide variety of life-defining behaviors, including cell migration, proliferation, and differentiation (1–4). The cellular cytoskeleton, which is the 3D network of biopolymers that defines cell structure and mechanics, plays a central role in processing these inputs and transducing them into intracellular biochemical signals. For example, the strong regulatory effect of extracellular matrix (ECM) stiffness on stem cell differentiation may be strongly modulated by activation or inhibition of myosin motors that tense the actin cytoskeleton (3, 5). While the molecular mechanisms of this cellular mechanobiology remain to be fully elucidated, there is widespread experimental support for a model in which cytoskeletal tension induces force-dependent conformational changes in specific mechanosensory proteins, which may in turn trigger signaling cascades through exposure of binding and phosphorylation sites (1, 6–13). Moreover, changes in cell and tissue mechanics frequently accompany specific disease states, including many solid tumors (14–18), and this correlation has spurred interest in exploring cellular mechanical properties as a biomarker. For all of these reasons, there is tremendous interest in developing precise ways of quantifying cellular mechanical properties. Traditionally, cellular mechanical properties such as elasticity are measured using single-cell rheological tools, such as atomic force microscopy (AFM), optical tweezers, and micropipette aspiration (19–21). Despite the fact that these approaches have lent much insight into the molecular basis of cellular mechanics, they are extremely skill intensive, require sophisticated technological equipment, and—most critically—are very low throughput. Moreover, these methods require that the cell be placed in highly artificial 2D culture paradigms that allow direct physical contact between the rheological probe and the cell. For this reason, there is a strong need for complementary technologies that enable measurement of cellular mechanical and migratory properties at higher throughput and in a manner that places cells in culture platforms that capture important physical features of tissue.

The application of microfluidic technology to the study of cellular mechanics and migration has the potential to address many of these needs. By leveraging precision fabrication technologies pioneered in the semiconductor and microchip industries, microfluidics and related soft lithographic approaches permit the creation of micrometer-scale devices in a reproducible, rapid, and inexpensive fashion. Importantly, the length scale accessible to this fabrication aligns well with cellular length scales, thus allowing the design and generation of engineered microenvironments for single cells that can capture salient physical features of tissue. For example, devices featuring microfluidic channels of <50 μm in width can be used to study the effect of confinement on cell motility (22, 23). Because such devices may be fabricated from a wide variety of materials, including polydimethylsiloxane (23, 24), polyacrylamide (PA) (25, 26), agarose (27, 28), and collagen (29), they can be tailored to present specific biochemical and mechanical signals to cells. Additionally, because many of these materials are transparent, cells within the resulting devices may be optically imaged in real time in ways that are often challenging in 3D biomaterials.

Microfluidic devices also facilitate cheaper and faster experimental studies. Parallel or multiplexed experiments can be conducted on a single device owing to the small footprint, and experiments require only small sample amounts. As a consequence, the throughput of these technologies far outpaces traditional cell mechanics measurements, facilitating statistical power capable of capturing heterogeneities present within complex cell populations and rapid sample processing times that bring clinical utility within the realm of possibility. For example, microrheological devices based on stretching of single cells within a microfluidic channel now enable measurement at rates

as high as 1,000 cells per second (30), which has in turn been applied to cancer diagnostics (31, 32), analysis of motility of leukemia cells (33), and mechanistic dissection of embryonic stem cell differentiation (34). By contrast, the throughput of traditional single-cell mechanics methods, such as AFM and optical tweezers, is often described in terms of tens of cells per day.

Finally, because of the characteristically small physical dimensions of microfluidic devices, they support well-defined laminar flows (i.e., very low Reynolds number) when perfused with aqueous solutions. As a consequence, the flow within the device is predictable and consistent to the point where the flow velocity and velocity gradient can be considered known and incorporated into the design of the experiment. These capabilities have great value for engineering microenvironments for the controlled study of cell motility. For example, by creating parallel flow streams with varying concentrations of a soluble cue that stimulates or suppresses cell motility, one may establish highly stable diffusion-mediated gradients perpendicular to the flow streamlines to drive directional cell migration (35–38). Additionally, these laminar flows can be used to spatially pattern device surfaces with ECM proteins and other adhesive proteins via adsorption from the flow stream (39–41).

This review describes the recent application of microfluidic platforms to the study of cellular mechanics and motility, moving from highly reductionist systems to living cells that interact with an ECM. We begin by discussing synthetic structures that have been developed to model physical aspects of cells and cellular responses to mechanical deformation, such as vesicles and droplets. Next, we focus on the use of microfluidic devices to characterize cells in suspension, including red blood cells (RBCs). Finally, we discuss the application of microfluidic technologies to the mechanobiology of adherent cells, with a specific emphasis on regulation of cell motility by ECM confinement.

ARTIFICIAL PARTICLES, DROPLETS, CAPSULES, AND VESICLES

Because of the structural complexity, heterogeneity, and complex functional properties of cell membranes and the cytoskeleton, it is extremely challenging to dissect how specific molecular components contribute to whole-cell mechanical properties based on studies with living cells. For animal cells, the membrane is in general a three-layered compound system (42). The center layer is composed of a phospholipid bilayer incorporated with an enormous diversity of critical transmembrane- and membrane-associated proteins, including pumps, channels, and receptors. Oligosaccharides (collectively termed the glycocalyx) that posttranslationally modify the constituent lipids form the outer layer. The glycocalyx is increasingly acknowledged to contribute strongly to cellular mechanics and mechanotransduction (43, 44). Coupled to the bilayer on the intracellular side to form the inner layer is the cytoskeleton, a viscoelastic and highly dynamic polymer network whose components are in a constant state of assembly and disassembly, and which generates force through the consumption of biochemical free energy (e.g., ATP and GTP hydrolysis) (45, 46). Comparatively rigid organelles within the cell (e.g., the nucleus) represent yet additional mechanical heterogeneities (47) and in some cases can dominate specific mechanobiological behaviors, such as migration through narrow tissue spaces (48–50). In living cells, all of these features are tightly regulated in both space and time, with external stimuli capable of rapidly altering membrane and cytoskeletal composition and mechanics. For these reasons, a variety of bottom-up approaches have been developed that seek to model cells with synthetic constructs composed of purified components. These reductionist entities often have controllable properties (i.e., size, deformability) that may be tuned to align with living cells while dispensing with the inherent complexity and unpredictability of living cells. These model systems are also simple enough to allow close convergence of complementary theoretical, numerical, and experimental approaches that would be unattainable with living cells.

Before reviewing biological cell mechanics studies that use microfluidic technology, we first discuss artificial small bodies in order of increasing complexity—particles, droplets, capsules, and vesicles. Particles and droplets, though lacking a distinct, enclosing layer and thus by definition unable to exhibit deformations like those of cellular membranes, nevertheless provide a starting point for understanding the role of hydrodynamic forces and deformability in physical phenomena relevant to cell migration. For the purposes of this review, we define particles as solid bodies of homogeneous composition that may be further distinguished as rigid or deformable. Particles of finite elastic modulus deform to a limited extent owing to viscous stresses; as the elastic modulus goes to infinity, no deformation occurs and the particle is considered rigid. Droplets, consisting of a homogeneous viscous fluid dispersed in a continuous surrounding immiscible fluid, can deform indefinitely in a hydrodynamic flow field. Surface tension at the fluid-fluid interface and the viscosity ratio between the internal viscosity and surrounding fluid viscosity are the physical parameters that determine droplet deformation.

Capsules and vesicles have been widely used to model cells because they possess structured interfaces that show more intricate mechanical behavior than is possible with surface tension and respectively capture the elasticity of the cytoskeleton and the constant area of the lipid bilayer. Capsules are enclosed structures consisting of a thin elastic membrane separating an internal substance from the external environment, usually a fluid. The capsule membrane can range from elastic solid-like to viscoelastic by including, in the latter case, a viscous contribution in the constitutive law describing the membrane. The elastic shear modulus is the key membrane property that dictates capsule deformation, along with the ratio of the internal fluid viscosity to external fluid viscosity for fluid-filled capsules. Unlike vesicles and RBCs, capsule membranes may be extensible. Although capsules can have a gelled core and additional properties, such as high resistance to area change, in this review we consider only initially spherical capsules with a polymeric membrane surrounding a liquid interior. Vesicles are deformable enclosures surrounding a liquid interior but with a membrane that consists of phospholipid molecules arranged into a bilayer structure. The important constraint imposed by the structure of the lipid bilayer is the very high cost of area dilation; therefore, vesicle membranes are considered incompressible (51), and, like RBCs, their membrane area is inextensible. Whereas polymeric capsule membranes resist shear deformation, a vesicle's lipid bilayer may be sheared freely. In contrast to droplets, the surface tension is not a material property of the vesicle membrane; rather, as lipids flow, the effective surface tension between neighboring lipids adjusts locally and globally to enforce constant surface area.

Particles and Droplets

Early scientific studies of hydrodynamic forces acting on suspensions were motivated primarily by understanding blood flow. Experiments of blood flow through capillaries revealed several interesting effects that were a result of the tendency of RBCs to migrate to the center of the capillary. Most famously, in small capillaries with diameters <300 μm, Fåhræus & Lindqvist observed a decrease in RBC concentration in the capillary with respect to the feed reservoir at high flow rates (Fåhræus effect; 52) and a decreasing effective viscosity (lower flow resistance) of the blood suspension with decreasing diameter [Fåhræus-Lindqvist effect (53); **Figure 1*a***]. Both effects are a result of the concentration of RBCs at the tube center, leaving a thin, cell-free plasma layer near the capillary wall. The Fåhræus effect can be explained from the higher mean velocity of the RBCs concentrated at the tube center compared with the surrounding plasma fluid; this decrease of tube hematocrit plus the lower flow resistance of the plasma layer near the wall explains the Fåhræus-Lindqvist effect (54). However, understanding of the physical explanation of RBC lateral migration that leads to the Fåhræus and Fåhræus-Lindqvist effects was advanced through

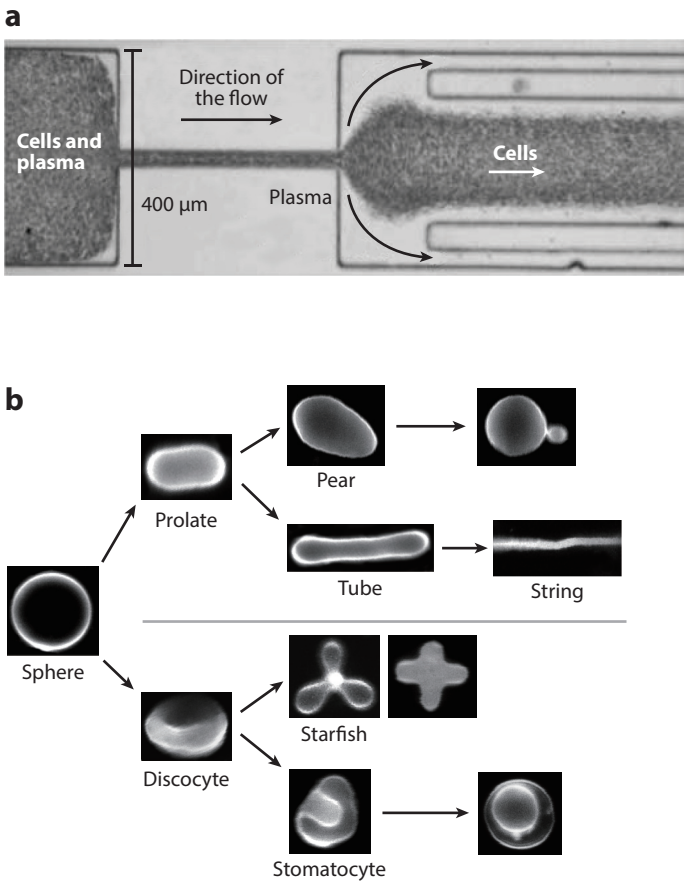

Figure 1

(*a*) Plasma-skimming microfluidic device that leverages the well-known cell-free layer phenomenon found in blood vessels. This lateral migration of red blood cells (RBCs) is partially responsible for the Fåhræus and Fåhræus-Lindqvist effects. Understanding of the physical mechanisms responsible for the lateral migration of RBCs to the channel center—hydrodynamic diffusion owing to collisional processes and lift forces that result from RBC deformability—was advanced through systematic studies of simpler suspensions of rigid particles and droplets. Reprinted with permission from Reference 164. Copyright 2006, IOS Press. (*b*) Synthetic vesicles exhibit a variety of shapes under different environmental conditions, including the discocyte and stomatocyte shapes often displayed by RBCs. Controlling the salt concentration, and therefore osmotic pressure difference between the vesicle and the surrounding aqueous solution, induced the shape deformation pathway of these synthetic vesicles. Reprinted with permission from Reference 78. Copyright 2008, American Physical Society.

systematic studies of simpler suspensions of rigid particles and droplets (55–71). This enhanced understanding of the origin of lateral migration has now been applied to applications such as sorting heterogeneous cell populations by size or deformability (cf. section on Circulating Cells).

Even the simple case of rigid, monodisperse, spherical particles suspended in a Newtonian fluid and flowing in a capillary exhibits surprisingly complex dynamics. In the limit of vanishing particle concentration (negligible particle-particle interactions) and vanishing inertial effects (i.e., for vanishing Reynolds number), the reversibility of Stokes flow means that particles will not migrate relative to the walls. However, concentrated suspensions of particles will migrate even

at vanishing Re as a result of shear-induced diffusion (57–61). In this case, gradients in the shear rate across the capillary lead to gradients in the particle collision frequency, which results in particles migrating away from the capillary walls and a layer depleted of particles forming adjacent to the walls. This hydrodynamic diffusion owing to collisional processes, along with lift forces that result from RBC deformability, contributes to the migration of RBCs responsible for the Fåhræus-Lindqvist effect.

At higher Re, inertial effects in the surrounding fluid induce sufficiently high lateral forces to allow rigid particles to migrate across streamlines even in the dilute limit. This phenomenon of inertial lateral migration across streamlines was first observed by Segré & Silberberg (55, 56), who found that uniformly distributed spherical particles at the inlet rearranged into a thin annular region further downstream for sufficiently high flow velocities and tube lengths. The basic inertial lift phenomenon is the following (62–65): Once the flow rate is high enough that fluid inertia must be taken into account, the disturbance to the fluid flow caused by the particle interacts with the wall and the curvature of the parabolic Poiseuille velocity profile. The particle's flow disturbance reflects at the wall, leading to an inward wall-induced inertial lift force directed toward the channel center. Further from the wall, the particle's flow disturbance interacts with the curvature in the velocity profile so that particles are pushed outward toward regions of higher shear rate closer to the walls. Sufficiently far down the channel, particles will have moved across the unidirectional streamlines to steady-state positions where the wall-induced and shear-gradient-induced inertial lift forces are equal. The inertial lift forces scale so predictably with particle size, channel geometry, and bulk flow velocity that microfluidic devices can be designed to separate heterogeneous populations of cells (discussed in the section on Circulating Cells). Indeed, the long entry lengths required for migration make microfluidic platforms ideal for both fundamental studies of migration and the exploitation of these phenomena for separations.

Although the potential importance of lateral inertial forces to cells likely can be understood from rigid particles, modeling the impact of cell membrane deformability on lateral migration requires the use of deformable objects. Droplets were the first deformable objects to be studied for lateral migration (66). In contrast to rigid particles that can migrate only across streamlines in channel flow owing to inertia-driven lift or shear-induced migration at finite concentrations, deformable droplets migrate even in creeping flow at vanishing concentration, as demonstrated experimentally (66, 67, 69, 72, 73). An expression for the lateral migration force on deformable drops is difficult to determine because the deformation of the droplet and the surrounding fluid flow are both unknown. Assuming weak deformation of the droplet, Chan & Leal (68) showed that the disturbance to the flow field induced by deformation of the droplet (that deformed the droplet in the first place) interacts with the wall and shear gradients to induce a lateral force on the droplet. The direction (toward or away from the channel center) and magnitude of this force depend on flow type (pressure-driven Poiseuille flow versus wall-driven Couette flow) as determined by channel geometry and the viscosity ratio of the droplet to surrounding fluid. The more complicated scenarios of large droplet deformation or several interacting droplets must be studied numerically (70, 71, 74). So once again the wall and shear gradients interact with the fluid disturbance. For rigid particles the disturbance occurs once fluid inertia is taken into account, and for droplets the disturbance is due to droplet deformation. More information about droplets is covered in two reviews about theoretical investigations (75) and experiments (76).

Capsules and Vesicles

Capsules and vesicles possess characteristics that facilitate our understanding of the behavior of individual RBCs flowing in the circulation, an important first step to understanding the collective behavior of whole blood. The RBC membrane exhibits approximately constant surface area and

has a nonspherical biconcave equilibrium shape, two characteristics that may be reproduced using vesicles. In particular, the discocyte–stomatocyte transition of RBCs is predicted by minimizing the lipid bilayer bending energy while changing the area-to-volume ratio (51), and this transition has been observed experimentally in vesicles (77, 78) (**Figure 1*b***). But the RBC cytoskeleton provides the cells with resistance to shearing forces, similar to an elastic capsule, leading to behavior that cannot be predicted from vesicles such as the echinocyte and elliptocyte shapes (79).

The manner in which capsules and vesicles each capture key mechanical aspects of RBCs is illustrated most clearly in shear flow. In shear flows, vesicles tumble end over end like a rigid axisymmetric particle (tumbling); tank-tread with a fixed ellipsoidal shape and inclination angle to the streamlines while the membrane rotates around the internal fluid, as seen for droplets (tank-treading); or tremble with an oscillating orientation and asymmetric shape distortion (trembling) at transition points that depend on shear stress strength and the viscosity ratio (80, 81). These experimental observations agree reasonably well with numerical predictions (82). Tumbling, tank-treading, and trembling have also been observed for RBCs (83, 84), though agreement of vesicle and RBC dynamic behavior is not as good at low shear rates as at higher shear rates (85). At moderate shear rates, RBCs demonstrate another dynamical motion between tumbling and tank-treading called swinging that is not seen for vesicles (83). In swinging, an oscillation of RBC inclination angle is superimposed over the tank-treading membrane rotation. This swinging motion has also been seen for capsules that have a slightly nonspherical resting shape (86). Thus, the swinging dynamics have been attributed to the shear elasticity and the elastic shape memory of the RBC cytoskeleton (83).

As with droplets, the deformable capsules and vesicles experience a lateral force in a confined channel even in creeping flow owing to the disturbance of a nonspherical deformed shape interacting with the channel walls (87–90) and the curvature of the velocity profile (91–95). But unlike droplets, for which the viscosity ratio determines the migration direction (68), vesicles and capsules always experience a lift force toward the channel center. The magnitude of the vesicle or capsule lateral migration velocity depends on viscosity ratio, geometry, local shear rate, and distance from the wall, with different expressions for near- and far-wall regimes (96). Once at the center of the channel, the capsules and vesicles are entrained in the fluid and move with approximately the maximum fluid velocity. In concentrated suspensions, this deformation-induced migration mechanism competes with the shear-induced diffusion mechanism described above to determine the thickness of the cell-free layer. As with the migration phenomena described in the section on Particles and Droplets, several microfluidic separation schemes based on deformation differences have been proposed (97–99), and experimental studies of the mechanism and scaling with flow and membrane parameters have relied on microfluidic platforms (92, 96, 100).

Just as vesicles have been used as a reductionist platform for understanding the mechanics of the lipid bilayer, purified and reconstituted proteins have been used to model and dissect the cytoskeleton. For instance, studies of reconstituted cytoskeletal networks have implied that prestress and stress-dependent stiffening of the cross-linked actin network are important contributors to cellular elastic behavior (101). In an effort to create a minimalist synthetic cell that can be used to study the interaction between the coupled lipid plasma membrane and the cytoskeleton and how that affects large-scale cell deformation, several researchers have recently reconstituted vesicles with encapsulated or surface-attached actin protein networks (102). One case of a vesicle-actin biomimetic system recapitulating cell behavior is the phenomenon of passive spreading on 2D surfaces. Vesicles with an actin cortex shell close to the inner membrane spread on histidine-coated glass substrates with a characteristic time in good agreement with early-time spreading dynamics of living cells (103). The accompanying modeling and analysis predicted the characteristic spreading time from the actin shell thickness and viscosity and the initial membrane tension.

Vesicles have been used to gain insight into physical aspects of cell adhesion, specifically to study the competition of attractive forces owing to cell adhesion molecule pairs, repulsive forces from other cell membrane proteins, and elastic membrane stresses determined by deformation of the cell membrane (104). Multicomponent vesicles with incorporated ligands that interact with receptors immobilized on a flat substrate have been used as a model system to study the weak, reversible adhesion that occurs before leukocytes or cancer cells become tightly attached to blood vessel walls (105–107). In one study, it was shown that the number of ligand-receptor bonds decreases steeply beyond a threshold of competitive antibody concentration, resulting in the de-adhesion of the vesicle (105). This experiment could lend mechanistic insight into how invasive tumor cells penetrate tissue; for example, many cancer cells overexpress metalloproteases that cleave glycoproteins, which then occupy potential ECM adhesion sites and facilitate continued motility through the tissue (104). Microfluidic techniques, which have yet to be widely used to study adhesion with these cell-mimetic systems, provide a means to study the effect of an external flow field on adhered cells, such as leukocytes that marginate from the bloodstream to adhere to vessel walls. Application of external flow can drive intramembrane flow of lipids within adherent vesicles (108), suggesting that shear applied to cells could facilitate the migration of specific adhesion proteins toward the contact zone, increasing the number of adhesion receptors and reinforcing the adhesion (84).

Although these artificial bodies have served as valuable model systems for cells, there are many other aspects of living cells that these model systems cannot capture, most notably the complexities of protein-based adhesion and signaling. Proteins can be incorporated within vesicle membranes to create some basal protein function and membrane heterogeneity (109), but they are unmoored from the signaling networks with which they would normally interface in living cells. These networks are critical for integrating the myriad physical and biochemical signals that are sensed by the cells and converted into biological responses. Thus, cells are able to actively respond to the environment—sensing conditions, processing information, and acting—whereas artificial bodies only deform in the presence of velocity gradients or chemical gradients.

CIRCULATING CELLS

Perhaps the most natural biological analogs to synthetic capsules and vesicles are cells that do not adhere to ECM surfaces, including those that flow within the vasculature. This includes both cells normally resident within blood, including RBCs and leukocytes, and cells associated with specific disease states. Of particular interest within the latter category are circulating tumor cells (CTCs), which are cells that shed from a solid tumor and may participate in seeding metastatic tumors. Because of the possibility of using CTC detection in blood-based diagnosis, screening, and monitoring, there is intense interest in developing technologies capable of identifying and measuring CTCs, a task made challenging by the high cellular background and comparative rarity of CTCs in blood. Microfluidic devices have been ideal for performing two clinical diagnostic tasks for circulating cells: high-throughput measurements of cell deformability and cell sorting.

RBCs have represented an important starting point for the application of mechanical tools. As alluded to earlier, mature RBCs consist of a phospholipid bilayer surrounding a fixed volume of cytosol with a known viscosity (110). Instead of a cytosol-filling cytoskeleton dominated by actomyosin bundles, microtubules, and intermediate filaments, RBCs have a simpler, mesh-like, spectrin-based cytoskeleton that is tethered to the intracellular face of the lipid bilayer (111). Additionally, RBCs do not contain a nucleus or other organelles, which facilitates the deformation of RBCs through narrow capillaries (110). As a result of their stereotypical and comparatively simplified structure and composition, RBCs have often been used as a model system to study

connections between molecular composition, cellular mechanics, and disease state. For example, malaria represents an RBC disorder whose progression has been closely linked to changes in mechanical properties. The malaria parasite invades and develops within a RBC through three stages: ring, trophozoite, and schizont. During the maturation process, the parasite produces its own proteins that interact with the lipid bilayer and the spectrin network, thereby rendering the RBC rigid, cytoadherent, and thus prone to occlusion within the narrow capillary beds (111, 112).

A variety of techniques have been applied to investigate the changes in the mechanical properties of the RBC experienced during disease progression, ranging from population-based approaches, such as viscometry and filtration-based approaches, to single-cell measurements, such as micropipette aspiration and optical tweezers. The individual cell measurements are of special interest owing to the fact that they can exert piconewton forces on micrometer length scales, both of which are highly relevant to a cell in vivo (113, 114). However, these techniques do not allow observation of RBCs flowing through narrow capillaries, which is of special importance because many of the clinical sequelae of malaria are directly associated with vaso-occlusion by infected RBCs (111). Additionally, the measurement throughput of these technologies is limited to several cells per hour, meaning the analysis of milliliter-volume samples for large population studies or clinical diagnosis is prohibitively time and labor intensive (115).

Microfluidic devices address the need for performing high-throughput RBC measurements in geometries that capture microvasculature geometry. In one study, a microfluidic device designed to mimic the geometry and elastic modulus of human capillaries was used to characterize RBC behavior of each malaria disease stage at high throughput (116) (**Figure 2*a***). In this device, RBCs were flowed through polydimethylsiloxane (PDMS) microchannels of widths of 2, 4, 6, and 8 μm in single file and at flow rates comparable to those observed in vivo. The first signs of rigidity occurred in the trophozoite stage, in which the infected cells were able to pass through the 6-μm and 8-μm channels but not the 2-μm and 4-μm channels (**Figure 2*b***). As the disease stage progressed, the cells became progressively rigid, with the shizont cells traversing only the 8-μm channels without difficulty. In this way, RBC flow could be conducted in a capillary-like geometry and at high throughput, which would not have been possible with micropipette aspiration or optical tweezers. Recent advances in microfluidic design and automated shape analysis have advanced the throughput of such approaches to 100–150 cells per second, which is orders of magnitude greater than previous single-cell technologies (117).

Acute myeloid leukemia is another disease that involves altered cell mechanics. In particular, the increased stiffness of leukemic cells, coupled with their increased adhesivity, leads to the aggregation of cells in the vasculature, called leukostasis. As with malaria, the resulting vaso-occlusion can contribute to organ failure. Rosenbluth and colleagues (118) devised an elegant AFM-based strategy to compare the stiffness of normal neutrophils, myeloid leukemia cells, and lymphoid leukemia cells and showed that the mean apparent equilibrium Young's modulus of the myeloid leukemia cells was substantially higher than that of either of the other two populations. In a follow-up study, the authors devised a capillary-mimetic microfluidic device to more directly investigate the consequences of these stiffness differences on flow behavior (119). Leukemic cells from a patient with leukostasis traversed the device more slowly and less frequently than cells from nonsymptomatic leukemia patients. The diseased cells occluded a higher fraction of the microchannels than the nonleukostatic cells, consistent with in vivo observations. Importantly, treatment of cells with drugs that induce cell softening significantly sped transit time, hinting at the power of such platforms for drug screening and validation.

More broadly, several other investigators have begun to investigate the mechanical properties of mammalian cells in a flow-based device. For example, a multistage PDMS device measured two biophysical intrinsic cell properties, cell size and deformability, of suspended heterogeneous cell

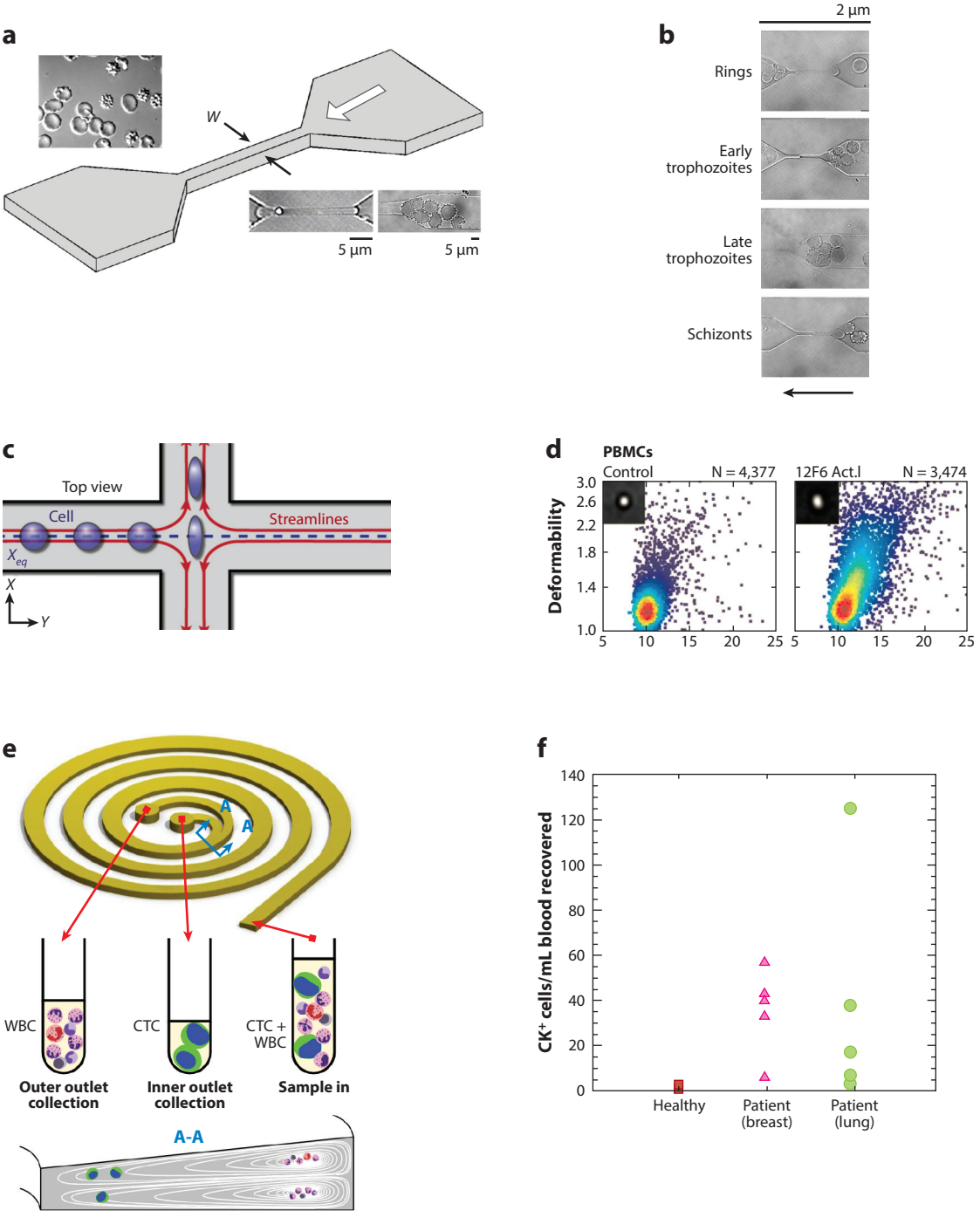

populations that could then be analyzed to predict metastatic potential, inflammation, stem cell state, and leukocyte activation (31). Suspended cells were ordered in the flow by inertial focusing and uniformly delivered to an extensional flow region, where they were elongated (**Figure 2*c***). With the use of a high-speed camera and rapid image processing, several thousand cells were observed and measured per second to yield a 2D size-deformability map of the population, which could be used as a quantitative signature of a given phenotype (**Figure 2*d***). For example, pleural fluid samples from a normal individual contained mostly small, rigid cells, which correspond to quiescent leukocytes. Samples from patients suffering from chronic inflammation contained more lymphocytes and histiocytes, which are larger and more deformable than leukocytes, therefore shifting the population median values. This device greatly increased the measurement throughput relative to conventional single-cell mechanics techniques (2,000 cells/s compared with 1 cell/min) and eliminated operator skill/bias issues and the need for biochemical labels.

Recently, many groups have begun to investigate and characterize the mechanics of CTCs owing to their clinical and biological significance. As described earlier, CTCs are tumor cells that have exited the primary tumor and entered the circulation. These CTCs are attractive clinical targets because they can be noninvasively sampled with venipuncture and could potentially be exploited for early detection, molecular profiling (e.g., sequencing and marker detection), and longitudinal disease monitoring. Additionally, genomic and proteomic analysis of CTCs can provide greater insight into the mechanism for metastasis or potential mechanisms for drug resistance (120). However, CTCs are extremely rare (estimated to be as few as 1 in 10^9 cells), and isolating these cells from the bloodstream is technically challenging (121). This problem of cell sorting has motivated much of the work of lateral migration of synthetic rigid and deformable particles discussed in the section on Artificial Particles, Droplets, Capsules, and Vesicles. One might reasonably expect that the scaling of lateral migration forces for deformable cells would follow predictions for rigid particles and deformable capsules, which would enable the design of cellular separation devices based on these predictions. As described below, flow-based microfluidic cell sorters use these lateral lift forces to separate cells based on size (e.g., CTCs are typically larger than other cells in the bloodstream) and deformability (e.g., healthy RBCs are softer than CTCs, white blood cells, and diseased RBCs).

Inertial migration separation devices leverage the fact that large particles laterally migrate to steady-state positions within the channel faster than smaller particles: For rigid particles, the lateral migration velocity is proportional to the cube of the diameter (122). Introducing changes to channel geometry along the flow direction introduces changes to the forces experienced by entrained particles with different size particles moving laterally at different speeds. One strategy

Figure 2

Microfluidic devices used to study circulating cells. (*a*) A microchannel device used to study the effect of malaria disease progression on red blood cells (RBCs). (*b*) As the disease progresses, RBCs are unable to deform and flow through a 2-μm-wide channel. Panels *a* and *b* adapted from Reference 116 with permission. Copyright 2003, National Academy of Sciences. (*c*) Probing the label-free biophysical marker of single-cell deformability with high-throughput hydrodynamic stretching. (*d*) Representative results of size versus deformability demonstrate the differences in deformability between the control and activated peripheral blood mononuclear cells (PBMCs). Panels *c* and *d* adapted from Reference 31 with permission. (*e*) A curved microchannel geometry with a trapezoidal cross-section creates large lateral separation between large and small particles, allowing for more concentrated lysed blood samples to be used. Smaller white blood cells and platelets are trapped in the Dean flow vortices near the outer wall, whereas the larger cancer tumor cells are pushed to the inner wall through a combination of inertial lift and Dean drag forces. This simple one-inlet, two-outlet device design is well suited for adaptation for a clinical assay. (*f*) Number of cancer tumor cells recovered per mL of prepared patient sample collected from healthy individuals (*red squares*), breast cancer patients (*pink triangles*), and lung cancer patients (*green circles*). 100% circulating tumor cell (CTC) detection from patient samples occurred at high capture efficiency (3–125 CTCs/ml) and throughput rates (~1 mL/h flow rates). Panels *e* and *f* reproduced from Reference 131 with permission. Abbreviation: WBC, white blood cell.

exploits this effect by modulating the channel aspect ratio (height-to-width ratio). One such two-stage inertial migration device (123) includes a high-aspect-ratio upstream segment in which the binary particle population equilibrates to certain positions followed by an expansion section to a low-aspect-ratio downstream segment with different equilibrium particle positions. The particles were collected at an intermediate point at which the large 20-μm particles had completed their migration to the center of the channel but the slower, small 9.9-μm particles largely remained at the channel walls. This approach enabled separation of this binary population with high efficiency and purity and could be used to detect and extract CTCs from spiked and diluted blood samples. Notably, although the device throughput was relatively high (100 μL/min) and produced efficient (>99%) and highly pure (>90%) particle separation, application of the approach to whole blood requires considerable (>40%) sample dilution to remain within the Newtonian regime and minimize cell-cell interactions; in practice, this may trade off against detection sensitivity. Another means of modulating channel geometry is to insert rectangular cavities at the channel sides that generate predictable vortices in which to trap CTCs (124–126). The sudden increase in channel width means the wall-induced lift effect diminishes and the shear-gradient-induced lift drives an outward migration of particles that scales as the cube of cell diameter (65). In this way, the large CTCs migrate into the cavities, whereas the smaller RBCs continue down the channel. A recent cavity vortex design demonstrated high-purity (80–100%) separation of CTCs from blood at high throughput rates (375 μL/min) and higher concentrations (5× –40× sample dilution) but suffered from low capture efficiency (10–35%) (126).

Curved microchannels have been shown to achieve separation at higher throughput (~1 mL/min) (122, 127, 128). In a curved microchannel geometry, a secondary flow induced by fluid inertia, called Dean flow, creates counter-rotating vortices and additional drag so that larger particles occupy a single equilibrium position at the inner wall and smaller particles are trapped in the core of the vortices at the center of the channel (122, 129). A trapezoidal cross-section increases the separation between large and small particles and cells owing to the asymmetry that skews the location of the vortex core toward the outer channel wall, allowing for more concentrated blood samples to be used (130). One device was able to analyze 2× diluted blood samples with high capture efficiency (~85%) for CTC-spiked blood samples and 100% CTC detection from patient samples at high capture rates (3–125 CTCs/mL) at ~1 mL/h flow rates (131) (**Figure 2*f***). This simple one-inlet, two-outlet device design is well suited for adaptation for a clinical assay (**Figure 2*e***).

An important remaining challenge for size-based separation techniques is the inability to separate CTCs that are similar in size to RBCs and other normal blood cells. In such cases, targeted trapping of CTCs on antibody-coated surfaces represents a promising approach but requires a high degree of mixing to drive CTCs toward the channel walls. Building upon advances in chaotic mixing in microfluidic channels (132), Stott and colleagues (121) produced a microfluidic herringbone design with ridges that induced chaotic motion of the blood sample. This device demonstrated high capture efficiency (85%) and sample purity, though at a lower throughput rate (1 mL/h) than the inertial separation devices. After separation, the captured CTCs remained viable and accessible for detailed in situ morphological analysis.

ADHERENT CELLS

In the previous sections, we discussed the use of microfluidic devices to study the mechanics and flow properties of nonadherent (e.g., circulating) cells and cellular mimics. At the same time, microfluidic devices lend themselves well to studies involving cells that normally adhere to other cells or ECM. As previously mentioned, many features in these devices can be precisely and reproducibly fabricated in the millimeter to micrometer range, which spans length scales on the

order of multiple cells to smaller than the diameter of a nucleus. These cell-relevant length scales allow the user to create pseudo-3D environments in which the cell physically contacts surfaces on all sides, as is often the case in tissue. This is unlike planar 2D culture surfaces commonly used in the laboratory (e.g., tissue culture polystyrene or glass coverslips), where cells contact the ECM only on the ventral surface and are freely bathed in medium on all other surfaces. Much recent work in a variety of cell and tissue systems has shown that this culture dimensionality can dramatically influence cell behavior, and it is often the case that encapsulation of cells within 3D environments more faithfully replicates behavior observed in tissue (2, 133, 134). One striking phenotypic difference between the two environments is the dominant mode of cellular migration.

Cell motility on 2D substrates has been extensively studied and modeled. Polarized signaling directs the formation of flat lamellipodial protrusions at the leading edge, adhesion to the substrate, and subsequent retraction at the trailing edge. However, in constrained 3D matrices, cells can adopt lamellipodium-independent migration phenotypes, such as those characterized by the formation of blunt-ended cylindrical extensions known as lobopodia (135). For example, a nuclear piston mechanism was recently proposed to describe lobopodial migration in confined 3D matrices (136). In this model, the front and rear of the cell are differentially pressurized, with the nucleus acting as the piston that can physically compartmentalize the cell. Actomyosin contractility is necessary to drive the nucleus forward to create these pressure differences. As expected, the compartmentalized pressure difference is not seen on unconfined cells on 2D substrates. The difference between 2D and 3D migration has been investigated extensively and is shown to be conserved across many different cell lines (23, 134, 137–139).

Confined Migration

Microfluidic devices are increasingly being exploited to create pseudo-3D confined microenvironments to investigate effects of confinement on cell behavior, specifically cellular motility related to cancer migration and progression. In particular, these devices have proven invaluable for studying the early stages of metastasis, the process through which tumors spread to distant organs and which is responsible for the majority of cancer deaths (140–142).

During invasion and metastasis, a tumor cell must be able to deform and squeeze through spaces that are on the subcellular and subnuclear length scale. As a result, this process requires dynamic changes in the organization of the cytoskeleton and cellular mechanics. Microfluidic devices are extremely useful models for investigating invasion and metastasis owing to their ability to create extremely small features that match the tight spaces that cells would need to navigate in vivo (22, 24, 143–146). To investigate how mechanical confinement can influence the migratory phenotype, various groups have created microfluidic devices with arrays of microchannels with a cross-section comparable to a cell size. With the microchannel design, the cells are in contact with ECM proteins and mechanical cues on their entire circumference, which mimics an in vivo 3D environment. Although relatively simple, the microchannel-based approach has allowed the discovery of novel migratory patterns and mechanisms that may lend insight into how cells navigate tissue spaces (24, 147).

One intriguing migratory pattern of confined cells is spontaneous persistent motility. This phenomenon has been observed in a device that consisted of arrays of PDMS microchannels connected to a central well for cell seeding (24) (**Figure 3*a*,*b***). With this device, the authors were able to observe hundreds of cells simultaneously and to quantify their velocity and persistence. Cells in these channels spontaneously migrated persistently in one direction over a long period of time (>12 h), and this phenomenon was conserved across various cell lines. This behavior is much different from 2D migration, where cells generally migrate in a random walk unless subject

to some external gradient (148). Persistent 3D migration may be relevant to in vivo situations where cancer cells have been observed to invade along heterogeneous structures in tissues such as lymphatic vessels or white matter tracts. Importantly, these insights were uniquely made possible through the use of a microfluidic channel and could not have been obtained with traditional 2D or 3D matrix systems or cellular invasion paradigms, such as transwell chambers.

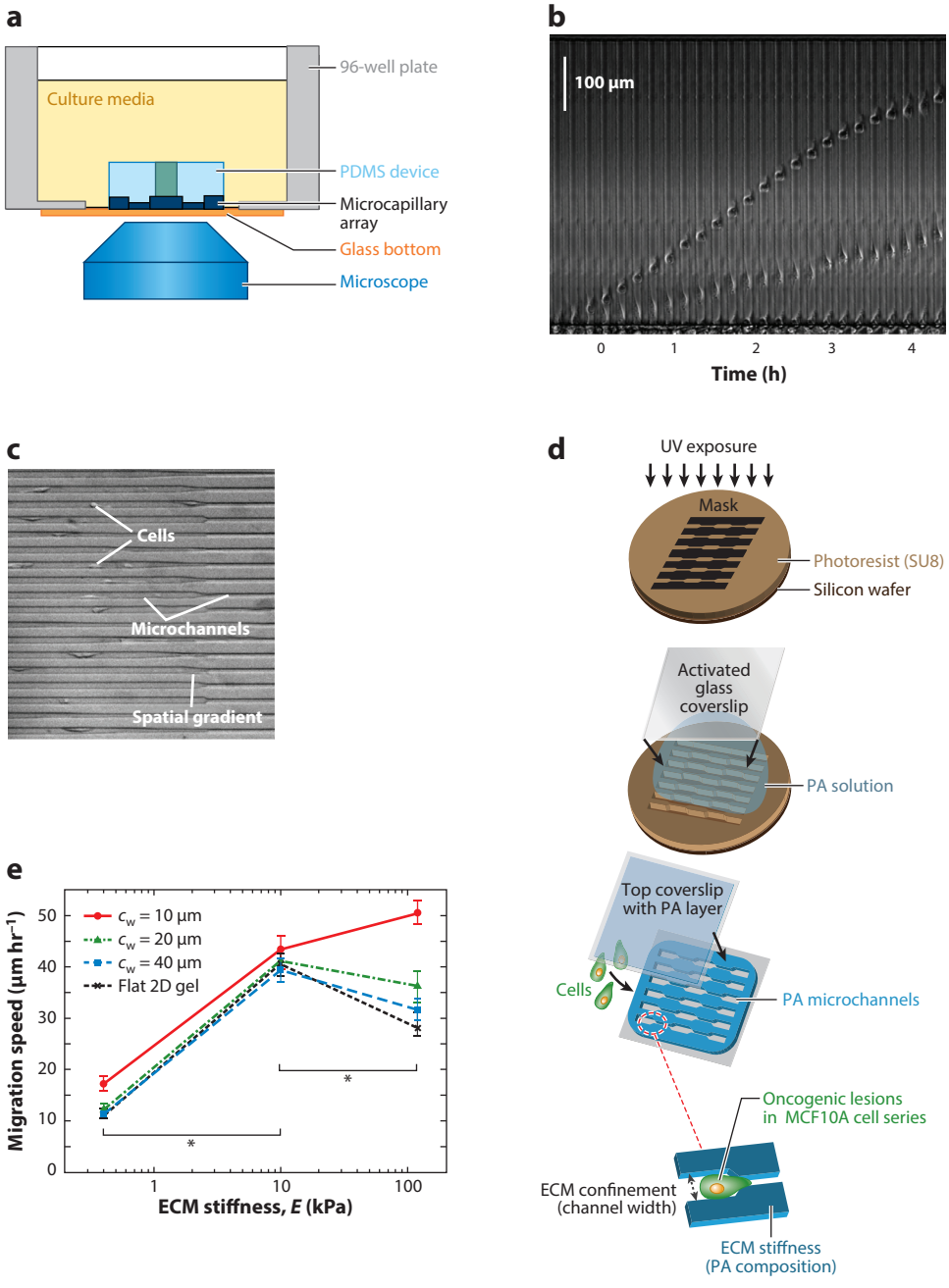

Microchannels have also been used to more closely examine mechanisms that underlie migration within confined tissue spaces. To induce cancer cells to migrate into and through microchannels, chemotactic gradients have been incorporated into microfluidic devices. In one such device (4, 23), two parallel microchannels bordering the migratory area were perfused with chemoattractant and empty medium, respectively. Through simple diffusion, a linear gradient formed perpendicular to the flow of the two media streams, and the cells were induced to enter the microchannels and directionally migrate. These investigations yielded multiple insights on the effect of confinement, such as the finding that confinement suppresses the mesenchymal phenotype normally observed in 2D migration by promoting uniform cytoskeletal tension and distribution of substrate adhesions, as well as a deeper understanding of the role of $\alpha 4\beta 1$ integrin signaling in myosin II–driven contractility for confined migration.

This chemotactic microfluidic platform has also been used to develop a novel mechanism for confined migration based on polarized transmembrane water permeation (147). In this model, a polarized cell establishes a gradient of plasma membrane proteins that features enrichment of the pump NHE-1 and aquaporin AQP5 at the leading edge of the cell. This polarization leads to a chemical potential difference across the membrane, which then results in a net inflow of water at the leading edge and a net outflow of water at the trailing edge, which leads to net cell displacement. The mechanism was tested experimentally by imposing external osmotic shocks and observing the direction of migration after the perturbation.

Many of the aforementioned devices use channels of constant width. However, tissue spaces may be expected to follow much more complex geometries, which may in turn strongly contribute to the speed and persistence of migration. There have been a variety of efforts to capture these effects. For example, microchannels that periodically taper from a cell width to subnuclear length scales have to been used to study cell metastasis (144, 145) (**Figure 3*c***). This periodic tapering both mimics the heterogeneity in ECM pore size and allows for multiple observations on the same cell in the same experiment. This platform led to the identification of four distinct phases for the subnuclear transition and quantification of the time spent in each phase. From these observations, multiple strategies used by the cell to cross the interface were identified: deforming the nucleus

Figure 3

Microfluidic devices for migration of adherent cells. (*a*) An example of a polydimethylsiloxane (PDMS)-based microfluidic device able to observe cell migration in a high-throughput manner with single-cell resolution. PDMS devices are placed in each well of a standard 96-well plate. By culturing individual wells according to different conditions and interfacing this device with a motorized microscope stage, one is able to measure multiple conditions in the same experiment. (*b*) Two cells, one with amoeboid and one with mesenchymal morphology, migrating in the same rectangular channel over a period of four hours. Solely owing to confinement, cells will spontaneously migrate in one direction. Panels *a* and *b* adapted from Reference 24, by permission of The Royal Society of Chemistry. (*c*) Periodically tapering channels better mimic cancer cell invasion through dense extracellular matrices (ECMs), where pore sizes can be on the subnuclear length scale. This design leads to the observation that multiple strategies are used by the cell to invade small spaces. These strategies include contraction of the cell so that the nucleus is deformed enough to pass through the small pore or slowly permeating the pore via rolling of the cell body. Reproduced from Reference 145 with permission. (*d*) To decouple the effect of stiffness and confinement on cell migration, polyacrylamide-based devices were fabricated with soft-lithography-based techniques. Stiffness is a property of the polyacrylamide (PA), whereas confinement is a property of the design. Adapted from Reference 150 by permission of The Royal Society of Chemistry. (*e*) Within these polyacrylamide-based devices, confinement in narrow channels (10-μm width) relieved the inhibitory effect of high stiffness that is seen in the larger channel widths. Adapted from Reference 22 with permission.

enough to pass through the barrier, using a cell body extension to elongate the cell body, or using a rolling motion to cross the barrier.

In the previous studies, the devices were made of PDMS. Although PDMS is ideal for recreating microscale topographic features, it offers a limited range of stiffness that does not fully cover the range of human tissue and microenvironment stiffness, including some stiffness ranges known to affect cellular phenotype (3, 22, 149). To cover a more physiologically relevant range of stiffnesses, researchers have created microfluidic devices using alternative materials with more tunable stiffness values, such as polyacrylamide. For example, one approach featured polyacrylamide microchannels with independently tunable stiffness and channel width, enabling deconvolution of effects of ECM stiffness and channel geometry (specifically, confinement) on cell motility (22) (**Figure 3*d***). This sort of deconstruction is not easily accomplished in 3D hydrogels, where mechanics and microstructure are often tightly coupled. For a given stiffness, cell migration speed increased with decreasing channel width. Moreover, whereas cells in wide channels slowed down at high stiffnesses, as has been observed previously on planar substrates, no such retardation of migration was observed in the narrowest channels, even at the highest stiffness (**Figure 3*e***). By combining these observations with confocal imaging of the actomyosin cytoskeleton and mathematical modeling, the authors deduced that confinement has the effect of polarizing traction forces and facilitating persistent motility. In a subsequent study, this platform was used to investigate the interplay of matrix stiffness and confinement with genetic lesions associated with malignant transformation in breast cancer (150).

Chemotaxis

In addition to providing a new set of tools to study cellular confinement, microfluidic devices are also well suited to study chemotaxis owing to the ability to create well-defined, stable concentration gradients. Chemotaxis, the directed migration in response to soluble extracellular cues, is essential for many biological processes, such as organ development, wound healing, and cancer metastasis (151). Specific chemokines have been implicated in tumor initiation, growth, and progression (152, 153). For example, perivascular niche–associated cells use autocrine factors such as SDF-1 to promote tumor malignancy, growth, and invasive potential (153). Additionally, SDF-1 can also contribute to cancer progression by stimulating tumor cell migration away from the primary tumor and to secondary sites away from the vasculature (152). Thus, various investigators have sought to replicate chemokine gradients in vitro to study cancer cell motility and invasion. Although several traditional in vitro chemotaxis systems do exist, including the Boyden, Zigmond, and Dunn chambers (39, 154) (**Figure 4*a***), the gradients generated by these devices are often poorly defined,

Figure 4

Microfluidic devices for chemotaxis. (*a*) A Boyden chamber is a popular nonmicrofluidic platform to measure chemotaxis. Cells are seeded in the upper compartment, and a chemokine is placed in the lower compartment. After several hours the number of cells that have migrated from the upper to lower compartment indicates how effective the chemokine is at inducing directional migration on a population level. However, the chemokine gradient is not steady and slowly decreases with time until equilibrium is reached. Adapted from Reference 154 by permission of The Royal Society of Chemistry. (*b*) A chemotactic microfluidic platform generates a steady chemokine gradient and allows for cell invasion measurements in known chemokine conditions. This device allows the direct comparison of cell migration behavior between the condition of interest and control sides. (*c*) Within the chemotactic microfluidic device, cell migration through 3D matrices can be studied under coculture conditions; MTLn3 cells are able to attract HMVEC cells, whereas limited invasion is seen on the control side (no cells seeded). Panels *b* and *c* adapted from Reference 155 by permission of The Royal Society of Chemistry.

unstable, and inaccessible to optical imaging. Microfluidic devices have offered the opportunity to complement and potentially improve upon these devices.

One such microfluidic device employed parallel flow channels packed with 3D collagen matrices (155–158) (**Figure 4*b***). A cell line of interest was seeded in one channel, and either a coculture of cells or chemokine-infused medium was added to the other channel (**Figure 4*c***). A linear

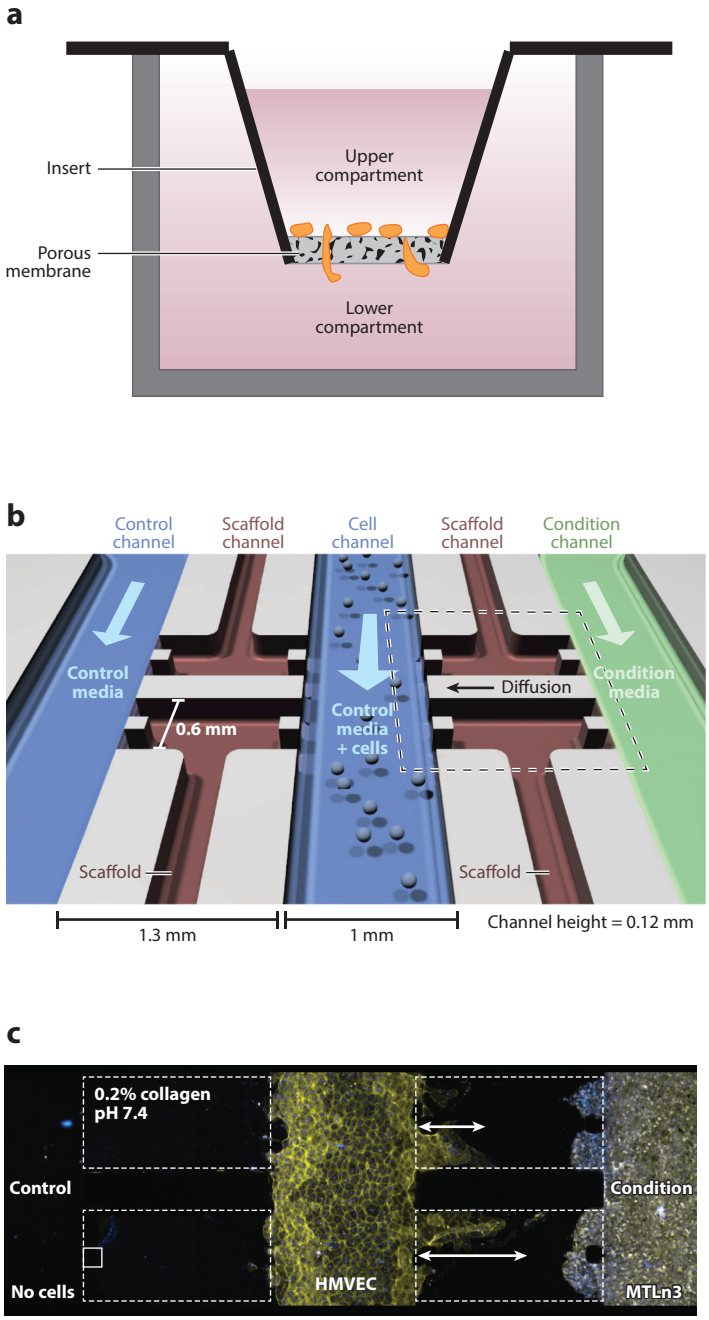

gradient was created and sustained either by the cocultured cells or by refreshing the chemokine-infused medium at regular intervals (158). These devices have been used to investigate the effect of matrix density on the epidermal growth factor–driven invasion of brain tumor cells (157). An important strength of this design is its modularity; one can easily change the type of matrix material, pore size, or stiffness of the matrix to investigate the effects of these parameters on invasive characteristics.

Many chemotactic processes do not involve a constant linear gradient of only one molecule, instead requiring a complex interplay of signals that vary in space and time (151). Additionally, the concentration of a chemokine can be locally degraded or sequestered, which further complicates the shape of the gradient. Examples of spatially heterogeneous gradients that have been incorporated into microfluidic devices are hill- and cliff-shaped gradients (38, 159) created by superimposing multiple linear gradients. In hill gradients, the concentration of chemokine gradually increases before gradually decreasing, whereas in cliff gradients the chemokine concentration gradually increases and then sharply drops. Unexpectedly, these two complex gradients produce dramatically different migratory behaviors. In the hill case, neutrophils were observed to migrate past the highest concentration of chemokine before reversing direction. However, in the cliff case, the neutrophils would stop migrating at the point of the highest concentration of chemokine. These behaviors are not easily explained by traditional models of chemotactic migration and suggest the presence of mechanisms whose details have yet to be elucidated. Additionally, this design represents a first step in creating more complex gradients that would be more physiologically relevant than a linear gradient.

CONCLUSION

Although the use of microfluidics to study cellular mechanics is still in its early stages, this suite of technologies has already proven to be a powerful tool for characterizing the mechanics of cells and cell-like particles quantitatively and at high throughput, and for gaining insight into microenvironmental regulation of cell migration. Such devices are beginning to make important contributions in the field of cellular mechanobiology, yet much room for improvement remains. For example, many of the devices presented to date focus on replication or manipulation of only one or two features of the microenvironment, such as confinement or a chemokine gradient. A challenging but important goal of future devices will be to incorporate multiple cues likely to play important roles in vivo, such as interstitial flow, topological cues, multiple different chemokine gradients, and more than one type of cell (160–162). Incorporation of these complexities will better capture the in vivo microenvironment and allow observation of emergent behaviors not readily appreciable from simpler systems. These devices will also lend insight into how cells process and integrate synergistic or competing cues to give rise to a coherent phenotype. Additionally, the integration of such devices with technologies that offer intracellular analysis, such as single-cell proteomic platforms (163), would increase the ability for endpoint analysis as well as archiving abilities for future analysis.

DISCLOSURE STATEMENT

The authors are not aware of any affiliations, memberships, funding, or financial holdings that might be perceived as affecting the objectivity of this review.

ACKNOWLEDGMENTS

We apologize to our many colleagues whose work could not be cited because of space limitations. This work was supported by grants from the National Science Foundation (1105539 to S.K., 1308051 to J.B.D., 1066334 to S.J.M.), the National Institutes of Health (R21CA174573 to S.K.; T32GM098218 training grant support to J.G.L.), and the W.M. Keck Foundation (Science and Engineering Grant to S.K.).

LITERATURE CITED

1. Ulrich TA, de Juan Pardo EM, Kumar S. 2009. The mechanical rigidity of the extracellular matrix regulates the structure, motility, and proliferation of glioma cells. *Cancer Res.* 69(10):4167–74
2. Rubashkin MG, Ou G, Weaver VM. 2014. Deconstructing signaling in three dimensions. *Biochemistry* 53(13):2078–90
3. Engler AJ, Sen S, Sweeney HL, Discher DE. 2006. Matrix elasticity directs stem cell lineage specification. *Cell* 126(4):677–89
4. Hung W-C, Chen S-H, Paul CD, Stroka KM, Lo Y-C, et al. 2013. Distinct signaling mechanisms regulate migration in unconfined versus confined spaces. *J. Cell Biol.* 202(5):807–24
5. Keung AJ, de Juan-Pardo EM, Schaffer DV, Kumar S. 2011. Rho GTPases mediate the mechanosensitive lineage commitment of neural stem cells. *Stem Cells* 29(11):1886–97
6. Felsenfeld DP, Schwartzberg PL, Venegas A, Tse R, Sheetz MP. 1999. Selective regulation of integrin-cytoskeleton interactions by the tyrosine kinase Src. *Nat. Cell Biol.* 1(4):200–6
7. Tamada M, Sheetz MP, Sawada Y. 2004. Activation of a signaling cascade by cytoskeleton stretch. *Dev. Cell* 7(5):709–18
8. Baneyx G, Baugh L, Vogel V. 2002. Fibronectin extension and unfolding within cell matrix fibrils controlled by cytoskeletal tension. *PNAS* 99(8):5139–43
9. Giannone G, Sheetz MP. 2006. Substrate rigidity and force define form through tyrosine phosphatase and kinase pathways. *Trends Cell Biol.* 16(4):213–23
10. Vogel V, Sheetz M. 2006. Local force and geometry sensing regulate cell functions. *Nat. Rev. Mol. Cell Biol.* 7(4):265–75
11. Margadant F, Chew LL, Hu X, Yu H, Bate N, et al. 2011. Mechanotransduction in vivo by repeated talin stretch-relaxation events depends upon vinculin. *PLOS Biol.* 9(12):e1001223
12. Lynch CD, Sheetz MP. 2011. Cellular mechanotransduction: filamin A strains to regulate motility. *Curr. Biol.* 21(22):R916–18
13. Schoen I, Pruitt BL, Vogel V. 2013. The yin-yang of rigidity sensing: how forces and mechanical properties regulate the cellular response to materials. *Annu. Rev. Mater. Res.* 43(1):589–618
14. Bissell MJ, Radisky DC, Rizki A, Weaver VM, Petersen OW. 2002. The organizing principle: microenvironmental influences in the normal and malignant breast. *Differentiation* 70(9–10):537–46
15. Paszek MJ, Zahir N, Johnson KR, Lakins JN, Rozenberg GI, et al. 2005. Tensional homeostasis and the malignant phenotype. *Cancer Cell* 8(3):241–54
16. Levental KR, Yu H, Kass L, Lakins JN, Egeblad M, et al. 2009. Matrix crosslinking forces tumor progression by enhancing integrin signaling. *Cell* 139(5):891–906
17. Egeblad M, Rasch MG, Weaver VM. 2010. Dynamic interplay between the collagen scaffold and tumor evolution. *Curr. Opin. Cell Biol.* 22(5):697–706
18. Ulrich TA, Jain A, Tanner K, MacKay JL, Kumar S. 2010. Probing cellular mechanobiology in three-dimensional culture with collagen-agarose matrices. *Biomaterials* 31(7):1875–84
19. Lee GYH, Lim CT. 2007. Biomechanics approaches to studying human diseases. *Trends Biotechnol.* 25(3):111–18
20. Huang H, Kamm RD, Lee RT. 2004. Cell mechanics and mechanotransduction: pathways, probes, and physiology. *Am. J. Physiol. Cell Physiol.* 287(1):C1–C11
21. Rodriguez ML, McGarry PJ, Sniadecki NJ. 2013. Review on cell mechanics: experimental and modeling approaches. *Appl. Mech. Rev.* 65(6):060801

22. Pathak A, Kumar S. 2012. Independent regulation of tumor cell migration by matrix stiffness and confinement. *PNAS* 109(26):10334–39
23. Balzer EM, Tong Z, Paul CD, Hung W-C, Stroka KM, et al. 2012. Physical confinement alters tumor cell adhesion and migration phenotypes. *FASEB J.* 26(10):4045–56
24. Irimia D, Toner M. 2009. Spontaneous migration of cancer cells under conditions of mechanical confinement. *Integr. Biol.* 1(8–9):506–12
25. Pathak A, Kumar S. 2011. Biophysical regulation of tumor cell invasion: moving beyond matrix stiffness. *Integr. Biol.* 3(4):267–78
26. Zaari N, Rajagopalan P, Kim SK, Engler AJ, Wong JY. 2004. Photopolymerization in microfluidic gradient generators: microscale control of substrate compliance to manipulate cell response. *Adv. Mater.* 16(23–24):2133–37
27. Haessler U, Kalinin Y, Swartz MA, Wu M. 2009. An agarose-based microfluidic platform with a gradient buffer for 3D chemotaxis studies. *Biomed. Microdevices* 11(4):827–35
28. Moffitt JR, Lee JB, Cluzel P. 2012. The single-cell chemostat: an agarose-based, microfluidic device for high-throughput, single-cell studies of bacteria and bacterial communities. *Lab Chip* 12(8):1487–94
29. Cheng S-Y, Heilman S, Wasserman M, Archer S, Shuler ML, Wu M. 2007. A hydrogel-based microfluidic device for the studies of directed cell migration. *Lab Chip* 7(6):763–69
30. Tse HTK, Gossett DR, Moon YS, Masaeli M, Sohsman M, et al. 2013. Quantitative diagnosis of malignant pleural effusions by single-cell mechanophenotyping. *Sci. Transl. Med.* 5(212):212ra163
31. Gossett DR, Tse HTK, Lee SA, Ying Y, Lindgren AG, et al. 2012. Hydrodynamic stretching of single cells for large population mechanical phenotyping. *PNAS* 109(20):7630–35
32. Remmerbach TW, Wottawah F, Dietrich J, Lincoln B, Wittekind C, Guck J. 2009. Oral cancer diagnosis by mechanical phenotyping. *Cancer Res.* 69(5):1728–32
33. Lautenschlaeger F, Paschke S, Schinkinger S, Bruel A, Beil M, Guck J. 2009. The regulatory role of cell mechanics for migration of differentiating myeloid cells. *PNAS* 106(37):15696–701
34. Chalut KJ, Hoepfler M, Lautenschlaeger F, Boyde L, Chan CJ, et al. 2012. Chromatin decondensation and nuclear softening accompany Nanog downregulation in embryonic stem cells. *Biophys. J.* 103(10):2060–70
35. Tong Z, Balzer EM, Dallas MR, Hung W-C, Stebe KJ, Konstantopoulos K. 2012. Chemotaxis of cell populations through confined spaces at single-cell resolution. *PLOS ONE* 7(1):e29211
36. Shamloo A, Ma N, Poo M-M, Sohn LL, Heilshorn SC. 2008. Endothelial cell polarization and chemotaxis in a microfluidic device. *Lab Chip* 8(8):1292–99
37. Saadi W, Wang S-J, Lin F, Jeon NL. 2006. A parallel-gradient microfluidic chamber for quantitative analysis of breast cancer cell chemotaxis. *Biomed. Microdevices* 8(2):109–18
38. Jeon NL, Baskaran H, Dertinger S, Whitesides GM, Van de Water L, Toner M. 2002. Neutrophil chemotaxis in linear and complex gradients of interleukin-8 formed in a microfabricated device. *Nat. Biotechnol.* 20(8):826–30
39. Keenan TM, Folch A. 2008. Biomolecular gradients in cell culture systems. *Lab Chip* 8(1):34–57
40. Jeon NL, Dertinger S, Chiu DT, Choi IS, Stroock AD, Whitesides GM. 2000. Generation of solution and surface gradients using microfluidic systems. *Langmuir* 16(22):8311–16
41. Fiddes LK, Chan HKC, Lau B, Kumacheva E, Wheeler AR. 2010. Durable, region-specific protein patterning in microfluidic channels. *Biomaterials* 31(2):315–20
42. Lodish H, Berk A, Zipursky SL, Matsudaira P, Baltimore D, Darnell J. 2000. *Molecular Cell Biology*. New York: W.H. Freeman. 4th ed.
43. Tarbell JM, Weinbaum S, Kamm RD. 2005. Cellular fluid mechanics and mechanotransduction. *Ann. Biomed. Eng.* 33(12):1719–23
44. Paszek MJ, DuFort CC, Rossier O, Bainer R, Mouw JK, et al. 2014. The cancer glycocalyx mechanically primes integrin-mediated growth and survival. *Nature* 511(7509):319–25
45. Fletcher DA, Mullins RD. 2010. Cell mechanics and the cytoskeleton. *Nature* 463(7280):485–92
46. Pullarkat P, Fernandez PA, Ott A. 2007. Rheological properties of the eukaryotic cell cytoskeleton. *Phys. Rep.* 449(1–3):29–53
47. Tseng Y, Kole TP, Wirtz D. 2002. Micromechanical mapping of live cells by multiple-particle-tracking microrheology. *Biophys. J.* 83(6):3162–76

48. Beadle C, Assanah MC, Monzo P, Vallee R, Rosenfeld SS, Canoll P. 2008. The role of myosin ii in glioma invasion of the brain. *Mol. Biol. Cell* 19(8):3357–68
49. Friedl P, Wolf K, Lammerding J. 2011. Nuclear mechanics during cell migration. *Curr. Opin. Cell Biol.* 23(1):55–64
50. Davidson PM, Denais C, Bakshi MC, Lammerding J. 2014. Nuclear deformability constitutes a rate-limiting step during cell migration in 3-D environments. *Cell. Mol. Bioeng.* 7(3):293–306
51. Seifert U. 1997. Configurations of fluid membranes and vesicles. *Adv. Phys.* 46(1):13–137
52. Fåhræus R. 1929. The suspension stability of blood. *Physiol. Rev.* 9(2):241–74
53. Fåhræus R, Lindqvist T. 1931. The viscosity of the blood in narrow capillary tubes. *Am. J. Physiol.* 96:562–68
54. Goldsmith HL, Cokelet GR, Gaehtgens P. 1989. Robin Fåhraeus: evolution of his concepts in cardiovascular physiology. *Am. J. Physiol.* 257(3):H1005–15
55. Segré G, Silberberg A. 1962. Behaviour of macroscopic rigid spheres in Poiseuille flow. Part 1. Determination of local concentration by statistical analysis of particle passages through crossed light beams. *J. Fluid Mech.* 14(01):115–35
56. Segré G, Silberberg A. 1962. Behaviour of macroscopic rigid spheres in Poiseuille flow. Part 2. Experimental results and interpretation. *J. Fluid Mech.* 14(1):136–57
57. Leighton D, Acrivos A. 1987. Measurement of shear-induced self-diffusion in concentrated suspensions of spheres. *J. Fluid Mech.* 177:109–31
58. Leighton D, Acrivos A. 1987. The shear-induced migration of particles in concentrated suspensions. *J. Fluid Mech.* 181:415–39
59. Nott PR, Brady JF. 1994. Pressure-driven flow of suspensions: simulation and theory. *J. Fluid Mech.* 275:157–99
60. Lyon MK, Leal LG. 1998. An experimental study of the motion of concentrated suspensions in two-dimensional channel flow. Part 1. Monodisperse systems. *J. Fluid Mech.* 363:25–56
61. Lyon MK, Leal LG. 1998. An experimental study of the motion of concentrated suspensions in two-dimensional channel flow. Part 2. Bidisperse systems. *J. Fluid Mech.* 363:57–77
62. Saffman PG. 1965. Lift on a small sphere in a slow shear flow. *J. Fluid Mech.* 22(2):385–400
63. Cox RG, Brenner H. 1968. The lateral migration of solid particles in Poiseuille flow—I theory. *Chem. Eng. Sci.* 23(2):147–73
64. Ho BP, Leal LG. 1974. Inertial migration of rigid spheres in 2-dimensional unidirectional flows. *J. Fluid Mech.* 65(Pt. 2):365–400
65. Di Carlo D, Edd JF, Humphry KJ, Stone HA, Toner M. 2009. Particle segregation and dynamics in confined flows. *Phys. Rev. Lett.* 102(9):094503
66. Goldsmith HL, Mason SG. 1962. The flow of suspensions through tubes. I. Single spheres, rods, and discs. *J. Colloid Sci.* 17(5):448–76
67. Goldsmith HL, Mason SG. 1961. Axial migration of particles in Poiseuille flow. *Nature* 190:1095–96
68. Chan PCH, Leal LG. 1979. The motion of a deformable drop in a second-order fluid. *J. Fluid Mech.* 92(01):131–70
69. Chan PCH, Leal LG. 1981. An experimental study of drop migration in shear flow between concentric cylinders. *Int. J. Multiphase Flow* 7(1):83–99
70. Zhou H, Pozrikidis C. 1994. Pressure-driven flow of suspensions of liquid drops. *Phys. Fluids* 6(1):80–94
71. Zhou H, Pozrikidis C. 1993. The flow of ordered and random suspensions of two-dimensional drops in a channel. *J. Fluid Mech.* 255:103–27
72. Karnis A, Mason SG. 1967. Particle motions in sheared suspensions: XXIII. Wall migration of fluid drops. *J. Colloid Interface Sci.* 24:164–69
73. Hiller W, Kowalewski TA. 1987. An experimental study of the lateral migration of a droplet in a creeping flow. *Exp. Fluids* 5:43–48
74. Zhou H, Pozrikidis C. 1993. The flow of suspensions in channels: single files of drops. *Phys. Fluids A Fluid Dyn.* 5(2):311–24
75. Rallison JM. 1984. The deformation of small viscous drops and bubbles in shear flows. *Annu. Rev. Fluid Mech.* 16:45–66

76. Stone HA. 1994. Dynamics of drop deformation and breakup in viscous fluids. *Annu. Rev. Fluid Mech.* 26:65–102
77. Berndl K, Käs J, Lipowsky R, Sackmann E, Seifert U. 1990. Shape transformations of giant vesicles: extreme sensitivity to bilayer asymmetry. *EPL* 13(7):659–64
78. Yanagisawa M, Imai M, Taniguchi T. 2008. Shape deformation of ternary vesicles coupled with phase separation. *Phys. Rev. Lett.* 100(14):148102
79. Sackmann E. 2006. Thermo-elasticity and adhesion as regulators of cell membrane architecture and function. *J. Phys. Condens. Matter* 18(45):R785–R825
80. Deschamps J, Kantsler V, Steinberg V. 2009. Phase diagram of single vesicle dynamical states in shear flow. *Phys. Rev. Lett.* 102(11):118105
81. Deschamps J, Kantsler V, Segre E, Steinberg V. 2009. Dynamics of a vesicle in general flow. *PNAS* 106(28):11444–47
82. Abreu D, Levant M, Steinberg V, Seifert U. 2014. Fluid vesicles in flow. *Adv. Colloid Interface Sci.* 208:129–41
83. Abkarian M, Faivre M, Viallat A. 2007. Swinging of red blood cells under shear flow. *Phys. Rev. Lett.* 98(18):188302
84. Abkarian M, Viallat A. 2008. Vesicles and red blood cells in shear flow. *Soft Matter* 4(4):653–57
85. Vlahovska PM, Podgorski T, Misbah C. 2009. Vesicles and red blood cells in flow: from individual dynamics to rheology. *C.R. Phys.* 10(8):775–89
86. Walter A, Rehage H, Leonhard H. 2001. Shear induced deformation of microcapsules: shape oscillations and membrane folding. *Colloids Surf. A Physicochem. Eng. Asp.* 183–85:123–32
87. Olla P. 1997. The lift on a tank-treading ellipsoidal cell in a shear flow. *J. Phys. II France* 7(10):1533–40
88. Callens N, Minetti C, Coupier G, Mader MA, Dubois F, et al. 2008. Hydrodynamic lift of vesicles under shear flow in microgravity. *EPL* 83(2):24002
89. Abkarian M, Lartigue C, Viallat A. 2002. Tank treading and unbinding of deformable vesicles in shear flow: determination of the lift force. *Phys. Rev. Lett.* 88(6):068103
90. Abkarian M, Viallat A. 2005. Dynamics of vesicles in a wall-bounded shear flow. *Biophys. J.* 89(2):1055–66
91. Kaoui B, Ristow GH, Cantat I, Misbah C, Zimmermann W. 2008. Lateral migration of a two-dimensional vesicle in unbounded Poiseuille flow. *Phys. Rev. E* 77(2):021903
92. Coupier G, Kaoui B, Podgorski T, Misbah C. 2008. Noninertial lateral migration of vesicles in bounded Poiseuille flow. *Phys. Fluids* 20(11):111702
93. Danker G, Vlahovska P, Misbah C. 2009. Vesicles in Poiseuille flow. *Phys. Rev. Lett.* 102(14):148102
94. Doddi SK, Bagchi P. 2008. Lateral migration of a capsule in a plane Poiseuille flow in a channel. *Int. J. Multiph. Flow* 34(10):966–86
95. Pozrikidis C. 2005. Numerical simulation of cell motion in tube flow. *Ann. Biomed. Eng.* 33(2):165–78
96. Geislinger TM, Franke T. 2014. Hydrodynamic lift of vesicles and red blood cells in flow—from Fåhræus & Lindqvist to microfluidic cell sorting. *Adv. Colloid Interface Sci.* 208:161–76
97. Hou HW, Bhagat A, Chong A, Mao P, Tan K. 2010. Deformability based cell margination—a simple microfluidic design for malaria-infected erythrocyte separation. *Lab Chip* 10(19):2605–13
98. Geislinger TM, Franke T. 2013. Sorting of circulating tumor cells (MV3-melanoma) and red blood cells using non-inertial lift. *Biomicrofluidics* 7:044120
99. Yang S, Lee SS, Ahn SW, Kang K, Shim W, et al. 2012. Deformability-selective particle entrainment and separation in a rectangular microchannel using medium viscoelasticity. *Soft Matter* 8(18):5011–19
100. Karimi A, Yazdi S, Ardekani AM. 2013. Hydrodynamic mechanisms of cell and particle trapping in microfluidics. *Biomicrofluidics* 7(2):021501
101. Gardel ML, Nakamura F, Hartwig JH, Crocker JC, Stossel TP, Weitz DA. 2006. Prestressed F-actin networks cross-linked by hinged filamins replicate mechanical properties of cells. *PNAS* 103(6):1762–67
102. Vogel SK, Schwille P. 2012. Minimal systems to study membrane. *Curr. Opin. Biotechnol.* 23(5):758–65
103. Murrell M, Pontani L-L, Guevorkian K, Cuvelier D, Nassoy P, Sykes C. 2011. Spreading dynamics of biomimetic actin cortices. *Biophys. J.* 100(6):1400–9
104. Sackmann E, Smith AS. 2014. Physics of cell adhesion: some lessons from cell-mimetic systems. *Soft Matter* 10:1644–59

105. Smith A-S, Lorz BG, Seifert U, Sackmann E. 2006. Antagonist-induced deadhesion of specifically adhered vesicles. *Biophys. J.* 90(3):1064–80
106. Smith A-S, Lorz BG, Goennenwein S, Sackmann E. 2006. Force-controlled equilibria of specific vesicle-substrate adhesion. *Biophys. J.* 90(7):L52–L54
107. Lorz BG, Smith A-S, Gege C, Sackmann E. 2007. Adhesion of giant vesicles mediated by weak binding of sialyl-Lewis^X to E-selectin in the presence of repelling poly(ethylene glycol) molecules. *Langmuir* 23(24):12293–300
108. Vezy C, Massiera G, Viallat A. 2007. Adhesion induced non-planar and asynchronous flow of a giant vesicle membrane in an external shear flow. *Soft Matter* 3(7):844–51
109. Girard P, Pécréaux J, Lenoir G, Falson P, Rigaud J-L, Bassereau P. 2004. A new method for the reconstitution of membrane proteins into giant unilamellar vesicles. *Biophys. J.* 87(1):419–29
110. Dao M, Lim CT, Suresh S. 2003. Mechanics of the human red blood cell deformed by optical tweezers. *J. Mech. Phys. Solids* 51(11–12):2259–80
111. Suresh S. 2006. Mechanical response of human red blood cells in health and disease: some structure-property-function relationships. *J. Mater. Res.* 21(8):1871–77
112. Cooke BM, Mohandas N, Coppell RL. 2001. The malaria-infected red blood cell: structural and functional changes. *Adv. Parasitol.* 50:1–86
113. Hochmuth RM. 2000. Micropipette aspiration of living cells. *J. Biomech.* 33(1):15–22
114. Zhang H, Liu K-K. 2008. Optical tweezers for single cells. *J. R. Soc. Interface* 5(24):671–90
115. Zheng Y, Nguyen J, Wei Y, Sun Y. 2013. Recent advances in microfluidic techniques for single-cell biophysical characterization. *Lab Chip* 13(13):2464–83
116. Shelby JP, White JM, Ganesan K, Rathod PK, Chiu DT. 2003. A microfluidic model for single-cell capillary obstruction by *Plasmodium falciparum*-infected erythrocytes. *PNAS* 100(25):14618–22
117. Zheng Y, Shojaei-Baghini E, Azad A, Wang C, Sun Y. 2012. High-throughput biophysical measurement of human red blood cells. *Lab Chip* 12(14):2560–67
118. Rosenbluth MJ, Lam WA, Fletcher DA. 2006. Force microscopy of nonadherent cells: a comparison of leukemia cell deformability. *Biophys. J.* 90(8):2994–3003
119. Rosenbluth MJ, Lam WA, Fletcher DA. 2008. Analyzing cell mechanics in hematologic diseases with microfluidic biophysical flow cytometry. *Lab Chip* 8(7):1062–70
120. Plaks V, Koopman CD, Werb Z. 2013. Circulating tumor cells. *Science* 341(6151):1186–88
121. Stott SL, Hsu C-H, Tsukrov DI, Yu M, Miyamoto DT, et al. 2010. Isolation of circulating tumor cells using a microvortex-generating herringbone-chip. *PNAS* 107(43):18392–97
122. Bhagat AAS, Kuntaegowdanahalli SS, Papautsky I. 2008. Continuous particle separation in spiral microchannels using Dean flows and differential migration. *Lab Chip* 8(11):1906–14
123. Zhou J, Giridhar PV, Kasper S, Papautsky I. 2013. Modulation of aspect ratio for complete separation in an inertial microfluidic channel. *Lab Chip* 13(10):1919–29
124. Zhou J, Kasper S, Papautsky I. 2013. Enhanced size-dependent trapping of particles using microvortices. *Microfluid. Nanofluid.* 15(5):611–23
125. Hur SC, Mach AJ, Di Carlo D. 2011. High-throughput size-based rare cell enrichment using microscale vortices. *Biomicrofluidics* 5(2):022206
126. Sollier E, Go DE, Che J, Gossett DR, O'Byrne S, et al. 2014. Size-selective collection of circulating tumor cells using Vortex technology. *Lab Chip* 14(1):63–77
127. Di Carlo D, Irimia D, Tompkins RG, Toner M. 2007. Continuous inertial focusing, ordering, and separation of particles in microchannels. *PNAS* 104(48):18892–97
128. Di Carlo D, Edd JF, Irimia D, Tompkins RG, Toner M. 2008. Equilibrium separation and filtration of particles using differential inertial focusing. *Anal. Chem.* 80(6):2204–11
129. Gossett DR, Di Carlo D. 2009. Particle focusing mechanisms in curving confined flows. *Anal. Chem.* 81(20):8459–65
130. Wu L, Guan G, Hou HW, Bhagat AAS, Han J. 2012. Separation of leukocytes from blood using spiral channel with trapezoid cross-section. *Anal. Chem.* 84(21):9324–31
131. Warkiani ME, Guan G, Luan KB, Lee WC, Bhagat AAS, et al. 2014. Slanted spiral microfluidics for the ultra-fast, label-free isolation of circulating tumor cells. *Lab Chip* 14(1):128–37

132. Stroock AD, Dertinger S, Ajdari A, Mezic I, Stone HA, Whitesides GM. 2002. Chaotic mixer for microchannels. *Science* 295(5555):647–51
133. Tibbitt MW, Anseth KS. 2009. Hydrogels as extracellular matrix mimics for 3D cell culture. *Biotechnol. Bioeng.* 103(4):655–63
134. Even-Ram S, Yamada KM. 2005. Cell migration in 3D matrix. *Curr. Opin. Cell Biol.* 17(5):524–32
135. Petrie RJ, Gavara N, Chadwick RS, Yamada KM. 2012. Nonpolarized signaling reveals two distinct modes of 3D cell migration. *J. Cell Biol.* 197(3):439–55
136. Petrie RJ, Koo H, Yamada KM. 2014. Generation of compartmentalized pressure by a nuclear piston governs cell motility in a 3D matrix. *Science* 345(6200):1062–65
137. Fraley SI, Feng Y, Krishnamurthy R, Kim D-H, Celedon A, et al. 2010. A distinctive role for focal adhesion proteins in three-dimensional cell motility. *Nat. Cell Biol.* 12(6):598–604
138. Zaman MH, Trapani LM, Sieminski AL, MacKellar D, Gong H, et al. 2006. Migration of tumor cells in 3D matrices is governed by matrix stiffness along with cell-matrix adhesion and proteolysis. *PNAS* 103(29):10889–94
139. Yamazaki D, Kurisu S, Takenawa T. 2009. Involvement of Rac and Rho signaling in cancer cell motility in 3D substrates. *Oncogene* 28(13):1570–83
140. Chambers AF, Groom AC, MacDonald IC. 2002. Metastasis: dissemination and growth of cancer cells in metastatic sites. *Nat. Rev. Cancer* 2(8):563–72
141. Yamaguchi H, Wyckoff J, Condeelis J. 2005. Cell migration in tumors. *Curr. Opin. Cell Biol.* 17(5):559–64
142. Fidler IJ. 2003. The pathogenesis of cancer metastasis: the "seed and soil" hypothesis revisited. *Nat. Rev. Cancer* 3(6):453–58
143. Jacobelli J, Friedman RS, Conti MA, Lennon-Dumenil A-M, Piel M, et al. 2010. Confinement-optimized three-dimensional T cell amoeboid motility is modulated via myosin IIA-regulated adhesions. *Nat. Immunol.* 11(10):953–61
144. Mak M, Reinhart-King CA, Erickson D. 2013. Elucidating mechanical transition effects of invading cancer cells with a subnucleus-scaled microfluidic serial dimensional modulation device. *Lab Chip* 13:340–48
145. Mak M, Reinhart-King CA, Erickson D. 2011. Microfabricated physical spatial gradients for investigating cell migration and invasion dynamics. *PLOS ONE* 6(6):e20825
146. Rolli CG, Seufferlein T, Kemkemer R, Spatz JP. 2010. Impact of tumor cell cytoskeleton organization on invasiveness and migration: a microchannel-based approach. *PLOS ONE* 5(1):e8726
147. Stroka KM, Jiang H, Chen S-H, Tong Z, Wirtz D, et al. 2014. Water permeation drives tumor cell migration in confined microenvironments. *Cell* 157(3):611–23
148. Wu P-H, Giri A, Sun SX, Wirtz D. 2014. Three-dimensional cell migration does not follow a random walk. *PNAS* 111(11):3949–54
149. Umesh V, Rape AD, Ulrich TA, Kumar S. 2014. Microenvironmental stiffness enhances glioma cell proliferation by stimulating epidermal growth factor receptor signaling. *PLOS ONE* 9(7):e101771
150. Pathak A, Kumar S. 2013. Transforming potential and matrix stiffness co-regulate confinement sensitivity of tumor cell migration. *Integr. Biol.* 5(8):1067–75
151. Roussos ET, Condeelis JS, Patsialou A. 2011. Chemotaxis in cancer. *Nat. Rev. Cancer* 11(8):573–87
152. Kedrin D, van Rheenen J, Hernandez L, Condeelis J, Segall JE. 2007. Cell motility and cytoskeletal regulation in invasion and metastasis. *J. Mammary Gland Biol. Neoplasia* 12(2–3):143–52
153. Rape A, Ananthanarayanan B, Kumar S. 2014. Engineering strategies to mimic the glioblastoma microenvironment. *Adv. Drug Deliv. Rev.* 79–80:172–83
154. Toetsch S, Olwell P, Prina-Mello A, Volkov Y. 2009. The evolution of chemotaxis assays from static models to physiologically relevant platforms. *Integr. Biol.* 1(2):170–81
155. Chung S, Sudo R, Mack PJ, Wan C-R, Vickerman V, Kamm RD. 2009. Cell migration into scaffolds under co-culture conditions in a microfluidic platform. *Lab Chip* 9(2):269–75
156. Jeong GS, Han S, Shin Y, Kwon GH, Kamm RD, et al. 2011. Sprouting angiogenesis under a chemical gradient regulated by interactions with an endothelial monolayer in a microfluidic platform. *Anal. Chem.* 83(22):8454–59
157. Zervantonakis IK, Chung S, Sudo R, Zhang M, Charest JL, Kamm RD. 2010. Concentration gradients in microfluidic 3D matrix cell culture systems. *Int. J. Micro-Nano Scale Transport* 1(1):27–36

158. Chung S, Sudo R, Vickerman V, Zervantonakis IK, Kamm RD. 2010. Microfluidic platforms for studies of angiogenesis, cell migration, and cell-cell interactions. *Ann. Biomed. Eng.* 38(3):1164–77
159. King KR, Wang S, Jayaraman A, Yarmush ML, Toner M. 2008. Microfluidic flow-encoded switching for parallel control of dynamic cellular microenvironments. *Lab Chip* 8(1):107–16
160. Kalchman J, Fujioka S, Chung S, Kikkawa Y, Mitaka T, et al. 2012. A three-dimensional microfluidic tumor cell migration assay to screen the effect of anti-migratory drugs and interstitial flow. *Microfluid. Nanofluid.* 14(6):969–81
161. Polacheck WJ, Charest JL, Kamm RD. 2011. Interstitial flow influences direction of tumor cell migration through competing mechanisms. *PNAS* 108(27):11115–20
162. Polacheck WJ, German AE, Mammoto A, Ingber DE, Kamm RD. 2014. Mechanotransduction of fluid stresses governs 3D cell migration. *PNAS* 111(7):2447–52
163. Kang C-C, Lin J-MG, Xu Z, Kumar S, Herr AE. 2014. Single-cell western blotting after whole-cell imaging to assess cancer chemotherapeutic response. *Anal. Chem.* 86(20):10429–36
164. Faivre M, Abkarian M, Bickraj K, Stone HA. 2006. Geometrical focusing of cells in a microfluidic device: An approach to separate blood plasma. *Biorheology* 43(2):147–59

Annual Review of Chemical and Biomolecular Engineering

Volume 6, 2015

Contents

A Conversation with Adam Heller
Adam Heller and Elton J. Cairns 1

An Integrated Device View on Photo-Electrochemical Solar-Hydrogen Generation
Miguel A. Modestino and Sophia Haussener 13

Synthetic Biology for Specialty Chemicals
Kelly A. Markham and Hal S. Alper 35

Chemical Looping Technology: Oxygen Carrier Characteristics
Siwei Luo, Liang Zeng, and Liang-Shih Fan 53

Gasification of Woody Biomass
Jianjun Dai, Jean Saayman, John R. Grace, and Naoko Ellis 77

Design Criteria for Future Fuels and Related Power Systems Addressing the Impacts of Non-CO_2 Pollutants on Human Health and Climate Change
James Jay Schauer 101

Graphene Mechanics: Current Status and Perspectives
Costas Galiotis, Otakar Frank, Emmanuel N. Koukaras, and Dimitris Sfyris 121

Smart Manufacturing
Jim Davis, Thomas Edgar, Robert Graybill, Prakashan Korambath, Brian Schott, Denise Swink, Jianwu Wang, and Jim Wetzel 141

Current Trends and Challenges in Biointerfaces Science and Engineering
A.M. Ross and J. Lahann 161

Defects in the Self-Assembly of Block Copolymers and Their Relevance for Directed Self-Assembly
Weihua Li and Marcus Müller 187

Clean Water for Developing Countries
Aniruddha B. Pandit and Jyoti Kishen Kumar 217

Thermoelectric Properties of Solution Synthesized Nanostructured Materials
Scott W. Finefrock, Haoran Yang, Haiyu Fang, and Yue Wu 247

Group Contribution Methods for Phase Equilibrium Calculations
Jürgen Gmehling, Dana Constantinescu, and Bastian Schmid 267

Microfluidic Strategies for Understanding the Mechanics of Cells and Cell-Mimetic Systems
Joanna B. Dahl, Jung-Ming G. Lin, Susan J. Muller, and Sanjay Kumar 293

Biocatalysis: A Status Report
Andreas S. Bommarius 319

Computational Modeling of Multiphase Reactors
J.B. Joshi and K. Nandakumar 347

Particle Formation and Product Formulation Using Supercritical Fluids
Željko Knez, Maša Knez Hrnčič, and Mojca Škerget 379

Indexes

Cumulative Index of Contributing Authors, Volumes 2–6 409

Cumulative Index of Article Titles, Volumes 2–6 412

Errata

An online log of corrections to *Annual Review of Chemical and Biomolecular Engineering* articles may be found at http://www.annualreviews.org/errata/chembioeng